

Electronic Supplementary Information

**Enhanced Ionic Photocurrent Generation through Homogeneous Graphene Derivative  
Composite Membrane**

*Yanbing Zhang<sup>1,2</sup>, Guoke Zhao<sup>3</sup>, Hongwei Zhu<sup>3</sup>, Lei Jiang<sup>1</sup>*

<sup>1</sup>CAS Key Laboratory of Bio-inspired Materials and Interfacial Science, Technical Institute of Physics and Chemistry Chinese Academy of Sciences, Beijing 100190, P. R. China

<sup>2</sup>University of Chinese Academy of Sciences, Beijing 100049, P. R. China

<sup>3</sup>State Key Lab of New Ceramics and Fine Processing, School of Materials Science and Engineering, Tsinghua University, Beijing 100084, P. R. China

**Materials and Methods**

Graphene oxide (GO) sheets (0.5-5  $\mu\text{m}$ ) and graphene oxide quantum dots (GOQDs) (diameter  $< 10$  nm) were purchased from Nanjing XFNANO Materials Tech Co., Ltd. PES microporous support was purchased from Beijing Tri-High Membrane Technology Co., Ltd. L-Ascorbic acid (LAA) was obtained from Sinopharm Chemical Reagent Co., Ltd. Sodium dodecyl benzene sulfonate (SDBS) was obtained from Sigma-Aldrich Chemical Co., Ltd. Other chemicals were analytical grade. The chemical reagents were used as received without further purification. Electrolyte solution was prepared with MilliQ water (18.2  $\text{M}\Omega\cdot\text{cm}$ ).

GO suspension was loaded into a 250 mL round bottom flask and sonicated to form a homogeneous dispersion, and then LAA and SDBS were added to the above light brown suspension. The mixture was refluxed under vigorous stirring in an oil bath at 50  $^{\circ}\text{C}$ . After 10 h, the suspension turned to black. The clear color change was apparent evidence that GO was reduced by LAA into rGO.<sup>1,2</sup>

Raman and X-ray photoelectron spectroscopy (XPS) spectra were recorded to characterize the changes in functional groups on GO sheets after reduction with LAA (Figure S1a). The  $I_D/I_G$  ratio of D ( $\sim 1595\text{ cm}^{-1}$ ) and G bands ( $\sim 1345\text{ cm}^{-1}$ ) implies the  $sp^3/sp^2$  ratio of carbon materials.<sup>3, 4</sup> Significantly increased  $I_D/I_G$  ratio verifies that GO was successfully reduced into r-GO.<sup>1, 3, 5</sup> The reduction of GO with LAA was also characterized using XPS (Figure S1b).<sup>1</sup> Before reduction, four types of carbon bonds, including C=C (284.7 eV), C-OH (286.4 eV), C (epoxide) (287.2 eV), and COOH (288.7 eV), were detected.<sup>6</sup> After reduction, the intensities of C (epoxide) peak decreased dramatically, revealing that most epoxy groups were removed.<sup>5</sup> This result further supports the reduction of GO by LAA.

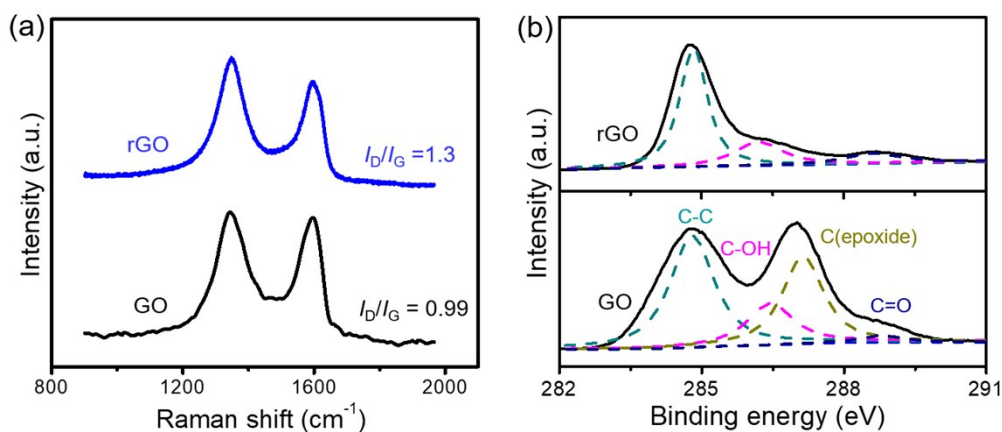


**Figure S1.** (a) Raman and (b) high resolution C1s XPS spectra of GO and rGO.

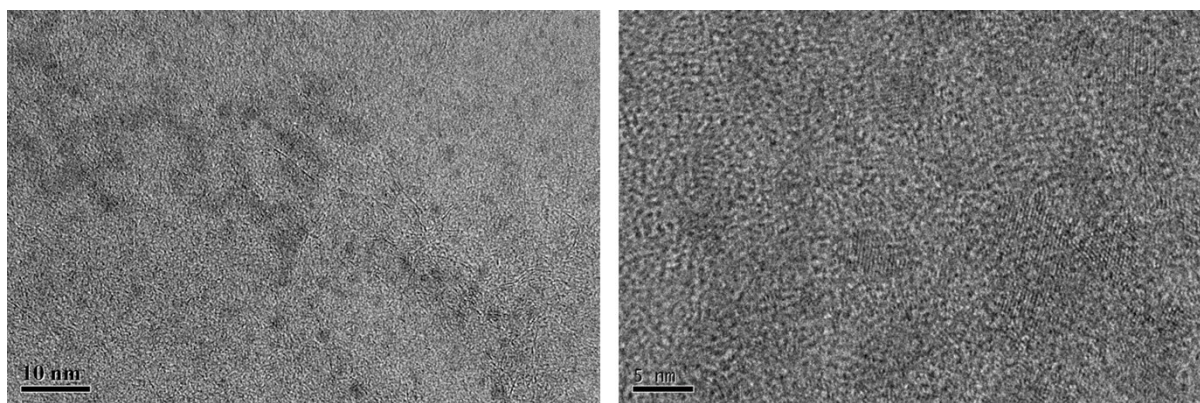


**Figure S2.** TEM images of a freestanding GOQDs/rGO membrane on a copper mesh.

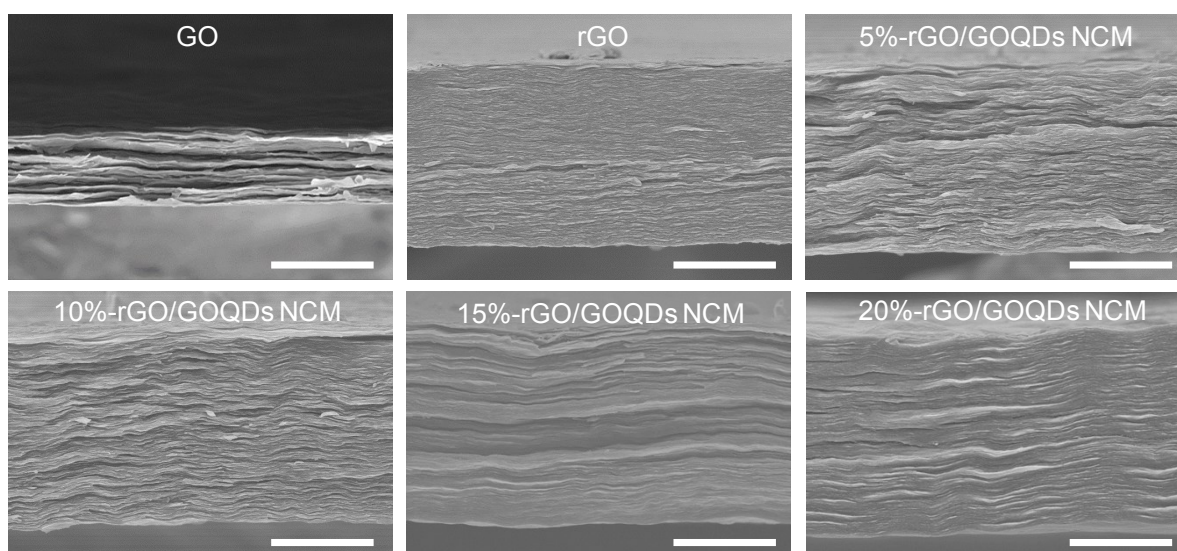


**Figure S3.** Cross-sectional SEM images of the membranes showing uniform packed lamellar structures (scale bars: 10  $\mu\text{m}$ ). Comparatively, the thickness of rGO film is increased to  $\sim 9.0$   $\mu\text{m}$  relative to  $\sim 3.8$   $\mu\text{m}$  of the GO film owing to the adsorption of L-tryptophan and sodium dodecyl benzene sulfonate. Furthermore, with increasing GOQDs content, the thickness mildly increased to 9.3  $\mu\text{m}$  for 20wt.% rGO/GOQDs NCM, indicating that the GOQDs were successfully embedded into the gallery between adjacent rGO sheets. All films contain the same amount of GO or rGO platelets.

GO and rGO colloids are negatively charged in water which was revealed by zeta potential measurements (Figure S4). At pH=6, the zeta potentials of GO and rGO are -53.23 and -45.6 mV, respectively.<sup>7</sup> It is assumed that the carboxylic groups cannot be reduced by LAA under the given reaction conditions.<sup>3</sup> These groups should therefore remain in the reduced product as confirmed by our XPS analysis (Fig. S1b). Furthermore, the magnitude of the zeta potential drops down with the increasing GOQDs' contents, resulting from increasing carboxyl groups of GOQDs.

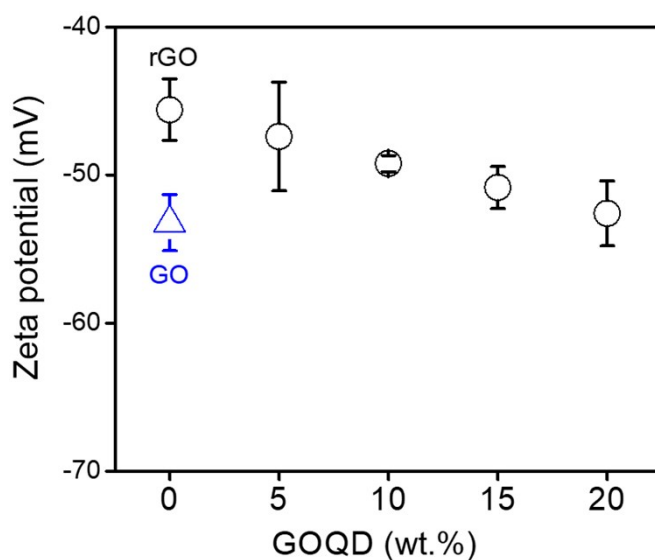


**Figure S4.** Zeta potential of GO and rGO colloids with different GOQDs contents (0.1 mg/mL) at pH=6. The zeta potential drops down with GOQDs' contents increasing.

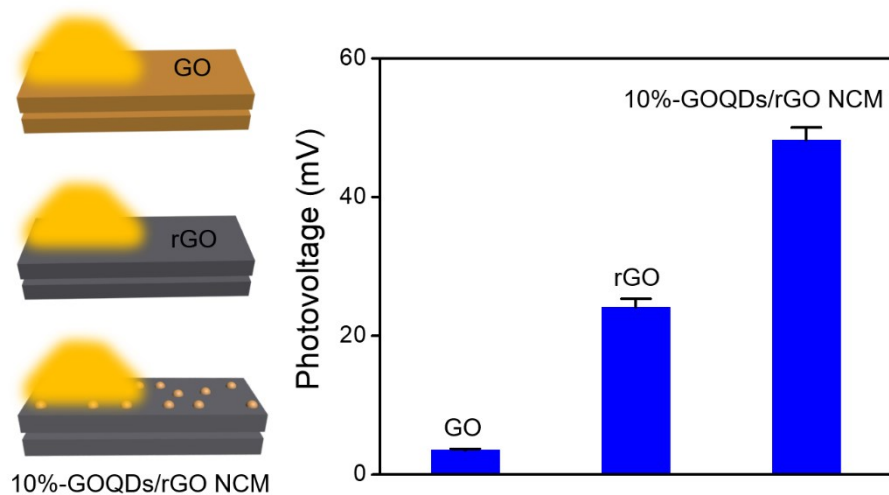


**Figure S5.** The photovoltage generated by dry membrane under light illumination (light intensity:  $\sim 60 \text{ mW/cm}^2$ , 20 s).

UV-vis absorption spectra of GO and rGO colloids with different GOQDs contents (0.02 mg/mL) at pH=6 was provided in Figure S6. Compared with GO dispersion, the photoabsorption of rGO dispersion is enhanced significantly. Furthermore, the absorption peak was red-shifted from 230 nm (GO dispersion) to 247 nm (rGO dispersion), suggesting that GO has been successfully reduced by LAA.<sup>8</sup> Besides, the absorbances of mixtures are slightly increased in contrast to rGO, irrelevant to the mass fraction of GOQDs. These results support that the photoabsorption increment of mixtures comes from rGO in comparison with GO.

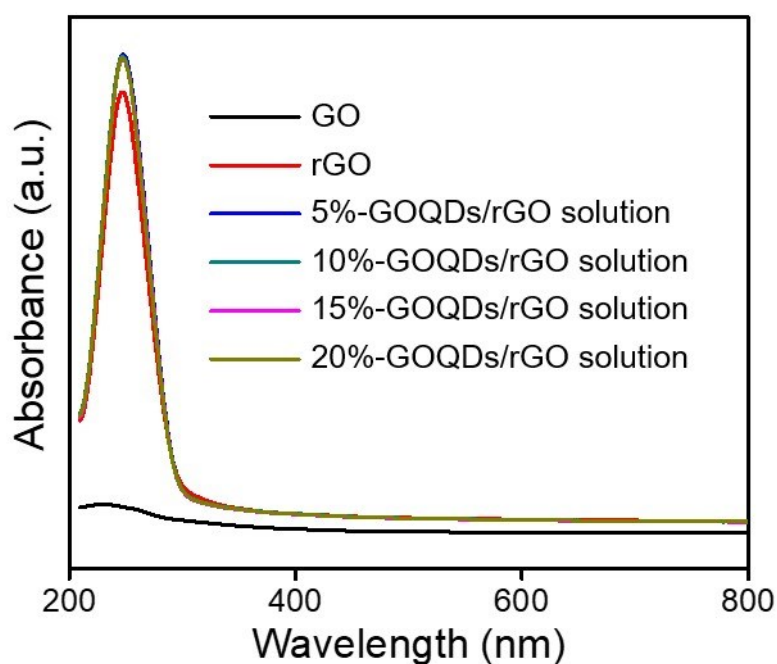


**Figure S6.** UV-vis absorption spectra of GO and rGO colloids with different GOQDs contents (0.02 mg/mL) at pH=6. Compared with GO dispersion, the photoabsorption of rGO dispersion is enhanced significantly. Besides, in contrast to rGO dispersion, the absorbances of mixtures are slightly increased, irrelevant to the mass fraction of GOQDs.

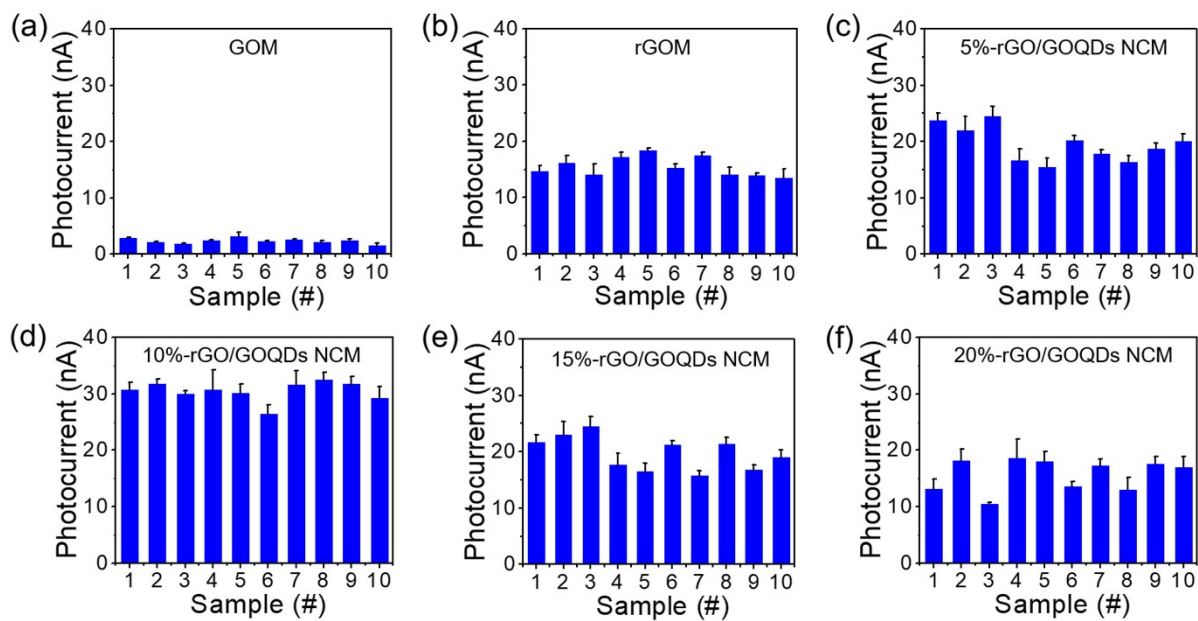


**Figure S7.** Ionic photocurrent of GOM and GOQDs/rGO NCM with different GOQDs contents measured on 10 separate devices. The light intensity was  $60 \text{ mW/cm}^2$ . The HCl concentration was  $1 \mu\text{M}$ .

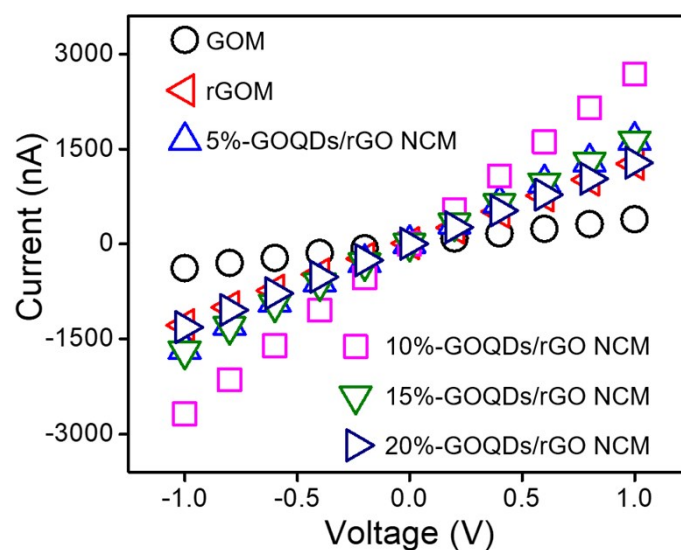


**Figure S8.** Current-voltage response of GOM and GOQDs/rGO NCM with different GOQDs mass fraction. With increasing contents of the GOQDs, the resulting ionic conductance experiences a rising trend at the beginning to achieve a maximum value at an intermediate GOQDs mass fraction about 10 wt.%, and then decrease sharply.

## References

1. J. Zhang, H. Yang, G. Shen, P. Cheng, J. Zhang and S. Guo, *Chem Commun (Camb)*, 2010, **46**, 1112-1114.
2. S. Pei and H.-M. Cheng, *Carbon*, 2012, **50**, 3210-3228.
3. J. Gao, F. Liu, Y. Liu, N. Ma, Z. Wang and X. Zhang, *Chem Mater*, 2010, **22**, 2213-2218.
4. T. Shen, D. Lang, F. Cheng and Q. Xiang, *Chemistryselect*, 2016, **1**, 1006-1015.
5. M. J. Fernandez-Merino, L. Guardia, J. I. Paredes, S. Villar-Rodil, P. Solis-Fernandez, A. Martinez-Alonso and J. M. D. Tascon, *J Phys Chem C*, 2010, **114**, 6426-6432.
6. J. Ji, Q. Kang, Y. Zhou, Y. Feng, X. Chen, J. Yuan, W. Guo, Y. Wei and L. Jiang, *Advanced Functional Materials*, 2017, **27**, 1603623.
7. B. Konkena and S. Vasudevan, *J Phys Chem Lett*, 2012, **3**, 867-872.
8. D. Li, M. B. Muller, S. Gilje, R. B. Kaner and G. G. Wallace, *Nat Nanotechnol*, 2008, **3**, 101-105.